Recurrence analysis of strange nonchaotic dynamics in driven excitable systems

E. J. Ngamga,[1] A. Buscarino,[2] M. Frasca,[2] L. Fortuna,[2] A. Prasad,[3] and J. Kurths[1]
[1]*Nonlinear Dynamics Group, Institute of Physics, University of Potsdam, Potsdam 14415, Germany*
[2]*Dipartimento di Ingegneria Elettrica Elettronica e dei Sistemi, Facoltà di Ingegneria, Università degli Studi di Catania, viale A. Doria 6, 95125 Catania, Italy*
[3]*Department of Physics and Astrophysics, University of Delhi, Delhi 110007, India*

(Received 11 October 2007; accepted 25 February 2008; published online 25 March 2008)

Numerous studies have shown that strange nonchaotic attractors (SNAs) can be observed generally in quasiperiodically forced systems. These systems could be one- or high-dimensional maps, continuous-time systems, or experimental models. Recently introduced measures of complexity based on recurrence plots can detect the transitions from quasiperiodic to chaotic motion via SNAs in the previously cited systems. We study here the case of continuous-time systems and experimental models. In particular, we show the performance of the recurrence measures in detecting transitions to SNAs in quasiperiodically forced excitable systems and experimental time series. © *2008 American Institute of Physics*. [DOI: 10.1063/1.2897312]

Like many other systems, excitable systems can show different responses depending on the kind of driving signal chosen to force them. In particular, it has been observed that, when the forcing is quasiperiodic, an excitable system can undergo transitions from quasiperiodic to chaotic behavior via a strange nonchaotic dynamics. In the strange nonchaotic regime, the system possesses strange (i.e., fractal) attractors but still has only a negative Lyapunov exponent, thus showing the nonchaotic behavior. Due to the negative Lyapunov exponent, two systems starting from arbitrary different initial conditions will converge to the same trajectory. We show that recently introduced measures of complexity based on the recurrence plots (RPs) allow one to detect transitions from quasiperiodic to chaotic motion via strange nonchaotic attractors (SNAs). Many electronic circuits showing chaotic dynamics have been derived from mathematical models based on nonlinear differential equations. In this paper, we present electronic implementations, based on operational amplifiers, of two different excitable systems both showing SNAs for particular values of the amplitude of the quasiperiodic forcing. Moreover, we apply recently introduced recurrence techniques based on RPs to the obtained experimental data. We show that recurrence measures are able to identify the transition to strange nonchaotic behavior in the experimental data.

I. INTRODUCTION

Excitable systems are omnipresent in nature. Excitable dynamics have been observed in various fields ranging from neuroscience, solid state physics, nonlinear optics, chemical reaction kinetics, to climate dynamics.[1–3] A system is said to be excitable if, for an external perturbation larger than a certain threshold value, the response of the system is independent of the size of the perturbation.[4] All forced excitable systems show a spiking behavior. They display the rest, firing, and recovery states. In the absence of perturbation, the system stays in the rest state. For a sufficiently strong perturbation, the system leaves the rest state, undergoes long excursions in phase space going through the excited and refractory states, before coming back to rest again. Many studies have been devoted to the effects of external noisy drivings on excitable systems.[5] It has been found that noise can induce various phenomena, such as oscillations, coherence resonance, stochastic synchronization, phase transitions, or spiral dynamics.[5,6] Quasiperiodic forcing could also play an important role in changing the dynamics in a system. Quasiperiodically forced nonlinear dynamical systems may exhibit SNAs which are objects lying between quasiperiodicity and chaos.[7] Mandell *et al.*[8] analyzed electroencephalogram data for signatures of SNAs and suggested that quasiperiodic driving may be a relevant internal mechanism for neuronal dynamics. Recently, Prasad *et al.*[9] studied the effect of quasiperiodic forcing in excitable systems. They found that the characteristic behavior of the spiking changes and strange nonchaotic or chaotic attractors are created. An experimental observation of SNAs in a driven excitable system made of an electromechanical cell has been realized.[10]

While some studies on SNAs have focused on the mechanisms through which SNAs appear in a system, others have focused on their characterization using tools such as Lyapunov exponents, spectral and geometrical properties, phase sensitivity and rational approximations, functional maps and invariant curves, as well as a renormalization-group analysis.[11,12]

Techniques based on recurrence plots have found applications in various fields.[13] In applications related to physics, the subjects of quasiperiodicity and chaos have been widely explored. For example, an analytic description of RPs and recurrence time statistics of chaotic processes have been done.[14,15] Zou *et al.* proposed procedures to distinguish quasiperiodic dynamics from chaos in short time series.[16,17] In a recent paper, we introduced measures of complexity based on the recurrence time and on a quantification of the syn-

chronization of trajectories on SNAs.[18] We showed the applicability of these measures on quasiperiodically forced maps and their robustness to additive noise. These measures are able to detect transitions, through different routes, from regular to chaotic motion via SNAs. Moreover, they identify the fractalization transition to SNAs, which most of the other tools of characterization fail to detect.

Our aim in this paper is to extend this study to continuous systems, particularly to excitable systems whose importance is well established in various fields.[5] Furthermore, we will also apply them to experimental data showing transitions to SNAs.

The paper is organized as follows. In the next section, we recall briefly the recurrence measures and apply them to two excitable models. Section III is devoted to the experimental realizations of both systems under study. In Sec. IV, we present the performance of the recurrence measures in detecting transitions to SNAs in these experimental data. The final section summarizes our results.

II. MEASURES OF COMPLEXITY APPLIED ON CONTINUOUS SYSTEMS

The basis of the measures of complexity to detect the transition from quasiperiodic to chaotic motion via SNAs is the recurrence plot (RP). RPs were introduced to visualize the time-dependent behavior of the dynamics of systems.[19] They allow us to see the recurrences of the phase-space trajectory to a certain state. In order to visualize these recurrences of a given trajectory $\{\vec{\mathbf{x}}_i\}_{i=1}^{N}$, one needs to compute an $N \times N$ matrix

$$R_{i,j} = \Theta(\delta - \|\vec{\mathbf{x}}_i - \vec{\mathbf{x}}_j\|), \quad i,j = 1, \ldots, N \tag{1}$$

where $\vec{\mathbf{x}}_i \in \mathbb{R}^n$, δ is a predefined threshold, $\Theta(\cdot)$ is the Heaviside function, and $\|.\|$ denotes a norm, here the maximum norm. The matrix compares the states of the system at times i and j. If the states are similar (δ-close), this is indicated by a 1 in the matrix. If on the other hand the states are rather different, the corresponding entry in the matrix is zero. The "1" and "0" are then, respectively, plotted as black and white points in a two-dimensional plot.[13] A reliable criterion for choosing the threshold has been proposed by Thiel *et al.*[20] They suggested that a measurement of an observation is the sum of the real signal and some observational noise with standard deviation. The threshold δ should be chosen five time larger than this standard deviation. We choose to normalize the data. This normalization leads the mean value of the data approximately to zero and their standard deviation σ to a range close to unity. We then choose the threshold $\delta = 0.04\sigma$. We have tried different values for the threshold and found other values leading to satisfactory results in the recurrence analysis.

Among the different lines and structures in the RP, we are interested in the "white vertical lines," whose length is equal to the time needed by the system to recur to a previously visited state. We evaluate the frequency distribution $P(w)$ of the lengths w of these white vertical lines. The first measure of complexity is then the mean of the distribution or, in other words, the mean recurrence time T_{MRT},

$$T_{\mathrm{MRT}} = \sum_{w=1}^{N} wP(w) \Big/ \sum_{w=1}^{N} P(w). \tag{2}$$

Another measure of complexity is the number of recurrences of the most probable recurrence time (N_{MPRT}). It is in fact the maximum value of the frequency distribution $P(w)$,

$$N_{\mathrm{MPRT}} = \mathrm{Max}(\{P(w)\}; \quad w = 1, \ldots, N). \tag{3}$$

It indicates how many times the system has recurred after the most probable recurrence time. We also consider the variance σ_{MRT} of T_{MRT} and σ_{MPRT} of N_{MPRT}. To compute the variances, a sufficiently long trajectory is considered and divided into l segments. T_{MRT} and N_{MPRT} are then computed for each segment separately. Thus

$$\sigma_{\mathrm{MRT}} = \frac{1}{l-1} \sum_{i=1}^{l} (T_{\mathrm{MRT}}(i) - \bar{T}_{\mathrm{MRT}})^2, \tag{4}$$

$$\sigma_{\mathrm{MPRT}} = \frac{1}{l-1} \sum_{i=1}^{l} (N_{\mathrm{MPRT}}(i) - \bar{N}_{\mathrm{MPRT}})^2, \tag{5}$$

where the overbar indicates the mean value.

Now we will apply this concept to excitable systems. We start with a system that models low–frequency fluctuations in a semiconductor laser with optical feedback:

$$\frac{dx}{dt} = y, \quad \frac{dy}{dt} = x - y - x^3 + xy + \epsilon_1 + \epsilon_2 x^2. \tag{6}$$

The dynamics of such systems has been extensively studied.[4,21] They present three types of dynamical behavior: time-independent intensity, low-frequency fluctuations, and coherent collapse regime. It has been shown that there is a range in the parameter space in which semiconductor lasers with optical feedback behave as excitable systems.[4,22] In the region of the parameter space where the system [Eq. (6)] behaves as an excitable system, three fixed points coexist: a repeller, a saddle, and a node. Their corresponding manifolds have the following behavior: the unstable manifold of the saddle is the stable manifold of the node, and the saddle is connected through its stable manifold with the repeller.[4]

A quasiperiodic forcing is applied to the system [Eq. (6)] by substituting ϵ_1 by $F(t)\epsilon_1$, where the modulation

$$F(t) = 1 + \epsilon(\cos t + \cos \omega t) \tag{7}$$

is quasiperiodic in time with the irrational frequency $\omega = (\sqrt{5}+1)/2$. This forcing changes the dynamics substantially. It has been shown that, depending on the value of the bifurcation parameter ϵ [Eq. (7)], some complex strange chaotic or nonchaotic attractors can be created.[9] The existence of the SNAs in which we are interested was confirmed by computing the largest Lyapunov exponent and the variance of a set of finite-time estimates of the Lyapunov exponent. It has been found that at the critical value $\epsilon \sim 5.02$ there is a drastic change in the fluctuations of the Lyapunov exponent indicating the transition from a quasiperiodic attractor to a SNA.[9]

Now, we apply our measures [Eqs. (2)–(5)] to the system given by Eq. (6). After computing the recurrence time measures, we observe in almost all the measures a drastic change

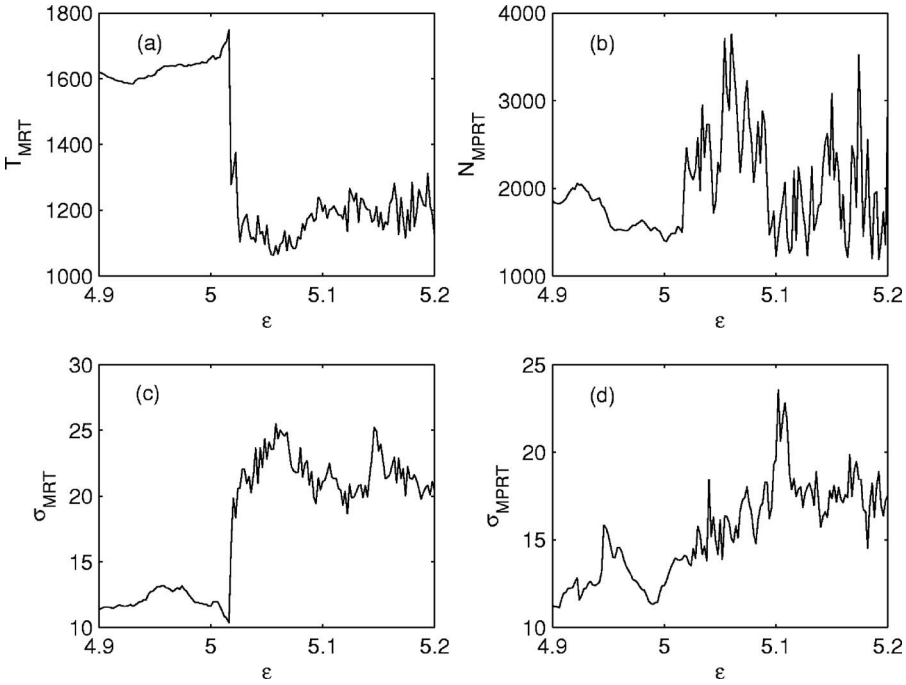

FIG. 1. Recurrence time measures, computed using numerically generated data of Eq. (6) with $\epsilon_1=0.08$ and $\epsilon_2=1$, vs bifurcation parameter ϵ [Eq. (7)]. The variances are computed with a trajectory of 300 000 data points and 1000 is the length of each segment. The threshold used is $\delta=0.04\sigma$, where σ is the standard deviation of the data. (a) Behavior of T_{MRT}; (b) behavior of N_{MPRT}; (c) variance of T_{MRT}; (d) variance of N_{MPRT}.

around the critical value $\epsilon\sim5.02$, confirming that the recurrence measures are able to detect the critical value at which the transition to SNAs takes place (Fig. 1). In addition, the fluctuations of the recurrence measures are clearly different before and after the critical value. T_{MRT} and N_{MPRT} are computed using 10 000 normalized data points. The variances are computed with a trajectory of 300 000 data points and 1000 is the length of each segment.

Next, we analyze the van der Pol–Fitz Hugh–Nagumo model (VdP–FHN), which is a paradigmatic excitable system. It models nerve pulses[1,23] and is described by the following equations:

$$\mu\frac{dx}{dt}=x-\frac{x^3}{3}-y,\quad \frac{dy}{dt}=x+\alpha. \tag{8}$$

The parameter α governs the character of solutions. For $|\alpha|>1$, the only attractor is a stable fixed point, and for $|\alpha|<1$ a limit cycle appears.[6] A quasiperiodic forcing is again introduced in the equations by substituting α by $F(t)\alpha$. This quasiperiodic forcing involves the creation of SNAs. A sudden increase in fluctuations of the Lyapunov exponent above $\epsilon\sim0.039$ has been found and shown to indicate a transition to a SNA.[9] This abrupt change is also observed in

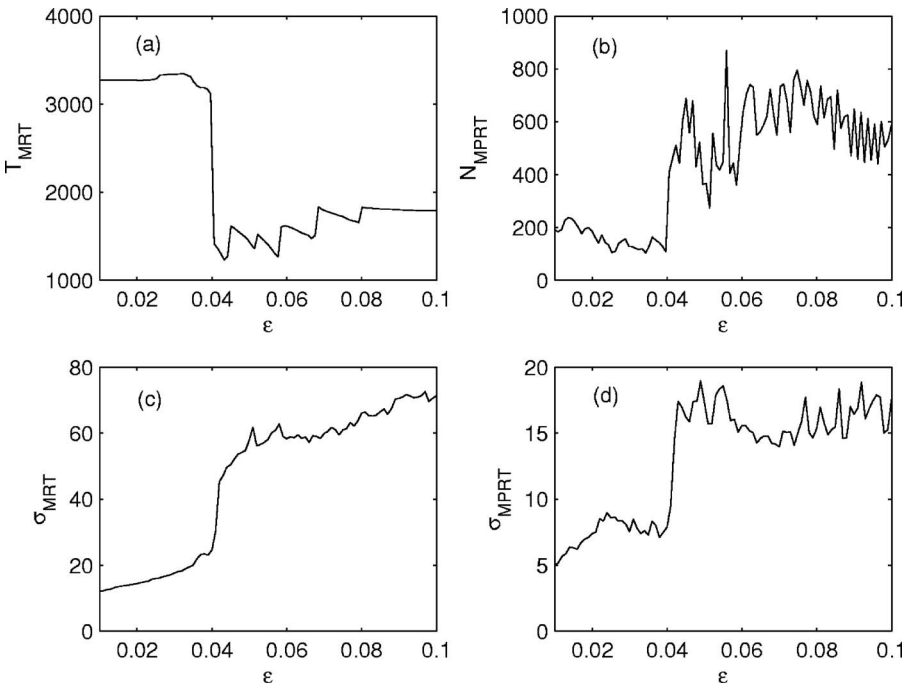

FIG. 2. Recurrence time measures, computed using numerically generated data of Eq. (8) with $\alpha=1.05$ and $\mu=0.01$, vs bifurcation parameter ϵ [Eq. (7)]. The threshold used is $\delta=0.04\sigma$, where σ is the standard deviation of the data. T_{MRT} and N_{MPRT} are computed using 10 000 normalized data points. The variances are computed with a trajectory of 300 000 data points and 1500 is the length of each segment. (a) Behavior of T_{MRT}; (b) behavior of N_{MPRT}; (c) variance of T_{MRT}; (d) variance of N_{MPRT}.

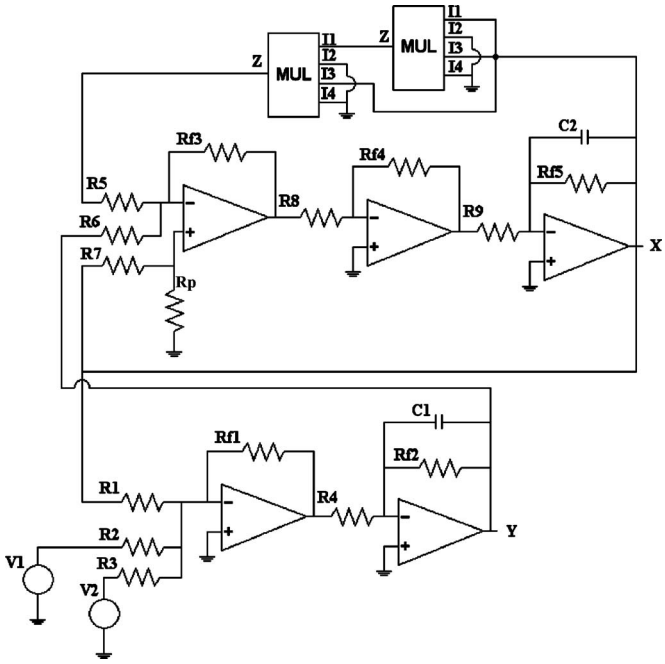

FIG. 3. Circuit 1: SNA circuit implementing Eq. (8) with $R_1=1$ kΩ, $R_2=952$ Ω, $R_3=952$ Ω, $R_4=10$ kΩ, $R_5=300$ Ω, $R_6=10$ kΩ, $R_7=10$ kΩ, $R_8=1$ kΩ, $R_9=10$ kΩ, $R_P=300$ Ω, $R_{f1}=1$ kΩ, $R_{f2}=100$ kΩ, $R_{f3}=10$ kΩ, $R_{f4}=10$kΩ, $R_{f5}=100$ kΩ, $C_1=235$ nF, and $C_2=27$ nF.

the recurrence time measures (Fig. 2). The measures fluctuate regularly in the quasiperiodic regime and rather strongly in the SNA regime. The crossover between these two regimes is abrupt, showing again the strong potential of the recurrence measures in detecting the transition.

III. IMPLEMENTATION OF SNA CIRCUITS

The existence of SNAs was first reported in the work of Grebogi *et al.*,[7] and then demonstrated in several physical systems, biological oscillators, and electronic circuits.[12] In particular, SNAs have been observed in electronic circuits made of an inductor, a capacitor, two or more resistors, and a nonlinear diode, such as Chua's diode, driven by quasiperiodic forcing.[24–26] Now we intend to implement electronic circuits of both models Eqs. (6) and (8) discussed in Sec. II. Therefore, we first rescale the dimensionless equations of the two previously considered models to achieve a realization of the circuits and we implement the rescaled equations by discrete-component circuits based on operational amplifiers.

A. Van der Pol–Fitz Hugh–Nagumo model

We first consider the VdP-FHN model. In our implementation, based on operational amplifiers, we associate the state variables x and y of Eq. (8) with voltages across two capacitors (C1 and C2 in Fig. 3, respectively) and we rewrite Eq. (8) as follows:

$$\mu\frac{dx}{d\tau}=k\left(x-\frac{x^3}{3}-y\right),\quad \frac{dy}{d\tau}=k(x+\alpha F(\tau)) \tag{9}$$

with $F(\tau)=1+\varepsilon(\cos k\omega_1\tau+\cos k\omega_2\tau)$ and $t=k\tau$. Although circuit implementation generally requires rescaling of both the state variables and the time variable, for our purpose only the time variable should be rescaled (by the factor k). Furthermore, let us define $\Omega_1=k\omega_1$ and $\Omega_2=k\omega_2$ as the frequencies of the sinusoidal waveforms used to build the driving signal $F(\tau)$ getting a SNA regime.

The circuit implementing Eq. (9) is shown in Fig. 3. It can be described by the following equations:

$$\begin{aligned}\frac{dx}{d\tau}&=k\frac{R_{f4}R_{f5}}{R_8R_9}\left(\frac{R_{f3}}{R_7}x-\frac{R_{f3}}{R_5}\frac{x^3}{100}-\frac{R_{f3}}{R_6}y\right),\\ \frac{dy}{d\tau}&=k\left(\frac{R_{f1}}{R_1}x+\frac{R_{f1}}{R_2}(1+\varepsilon\cos\Omega_1\tau)+\frac{R_{f1}}{R_3}\varepsilon\cos\Omega_2\tau\right),\end{aligned} \tag{10}$$

which, with the choice of the components reported in Fig. 3, match Eq. (9) with $k=1000$. In more details, we have set $\mu=R_8R_9/R_{f4}R_{f5}$, $R_{f3}/R_7=1$, $R_{f3}/100R_5=1/3$, $R_{f3}/R_6=1$, $R_{f1}/R_1=1$, $R_{f1}/R_2=R_{f1}/R_3=\alpha$. R_P was chosen to satisfy the gain rule,[27] $1/R_{f3}+1/R_5+1/R_6=1/R_7+1/R_P$. To implement the nonlinearity of the circuit, two AD633 multipliers have been used. These devices have four inputs (I_1,I_2,I_3,I_4) which are linked to the output by the following relationship: $Z=(I_1-I_2)(I_3-I_4)/10$. The two cascaded multipliers shown in Fig. 3 implement the nonlinearity $x^3/100$.

Finally, as integrators we used operational amplifiers into a Miller configuration.[27] The integrator block has been designed by following standard guidelines.[27] TL084 operational amplifiers are used and the power supply has been set to $\pm 15V$.

Figure 4 shows the projection of the attractor obtained experimentally from the circuit and the trend of the state variable $x(\tau)$ for parameter values such that the circuit is in the SNA regime. In particular, the parameters of the model have been chosen according to Ref. 9 $\alpha=1.05$, $\mu=0.01$, $\omega=(\sqrt{5}+1)/2$, $\varepsilon=0.1$.

B. Laser system

The second SNA circuit was designed starting from the dimensionless Eq. (6) and rewriting them in terms of a new rescaled time variable $(\tau=t/k)$ as

$$\frac{dx}{d\tau}=ky,\quad \frac{dy}{d\tau}=k(x-y-x^3+xy+\varepsilon_1F(\tau)+\varepsilon_2x^2), \tag{11}$$

with $F(\tau)=1+\varepsilon(\cos k\omega_1\tau+\cos k\omega_2\tau)$ and $\Omega_1=k\omega_1$, $\Omega_2=k\omega_2$. Even in this case, in fact, the discrete component circuit implementation based on operational amplifiers allows the dynamic range of the original state variables to be implemented without the need to rescale them.

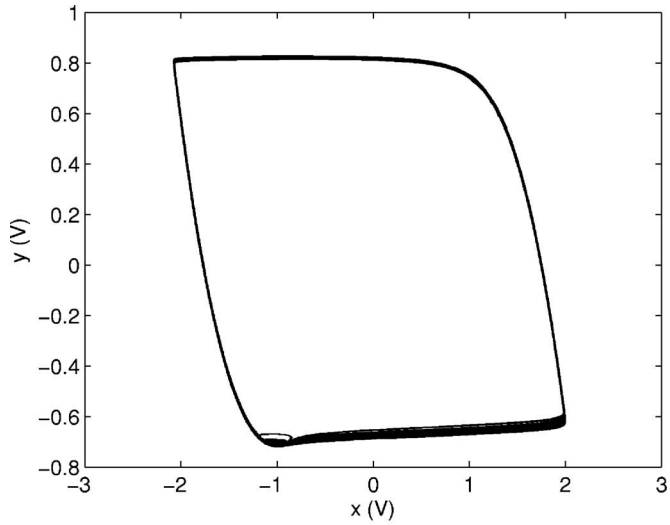

(a)

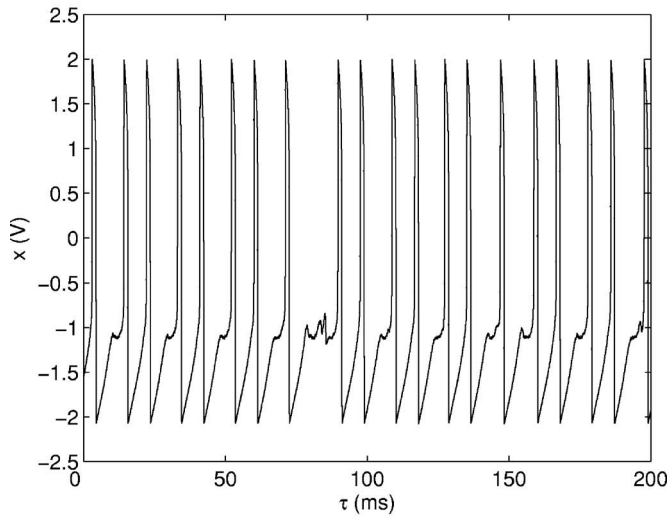

(b)

FIG. 4. Experimental results for Circuit 1 with $\varepsilon=0.1$. (a) Projection of the strange nonchaotic attractor in the phase plane x-y; (b) trend of the state variable $x(\tau)$.

The corresponding circuit is shown in Fig. 5. The state variables x and y are associated with voltages across the capacitors $C2$ and $C1$, respectively. The circuit is governed by the following equations:

$$\frac{dx}{d\tau}=k\frac{R_{f3}}{R_9}y,$$

$$\frac{dy}{d\tau}=k\left(\frac{R_{f2}}{R_7}\left(\frac{R_{f1}}{R_3}x+\frac{R_{f1}}{R_2}\frac{xy}{10}+\frac{R_{f1}}{R_4}\varepsilon_1(1+\varepsilon\cos\Omega_1\tau)+\frac{R_{f1}}{R_5}\varepsilon_1\varepsilon\cos\Omega_2\tau+\varepsilon_2\frac{R_{f1}}{R_1}\frac{x^2}{10}\right)-\frac{R_{f2}}{R_6}\frac{x^3}{100}-y\right), \tag{12}$$

which match Eq. (11) with the choice of parameters reported in Fig. 5. In particular, we have set $R_{f2}/R_7=1$, $R_{f1}/R_3=1$, $R_{f1}/R_2=10$, $R_{f1}/R_4=R_{f1}/R_5=1$, $R_{f1}/R_1=10\varepsilon_2$, $R_{f2}/R_6=100$, $R_{f3}/R_9=1$.

The nonlinearities of the system x^3 and xy are implemented with three AD633 multipliers. An operational amplifier and a RC filter have been used to perform the integration of the two state variables x and y, respectively. Their parameters have been fixed following standard guidelines[27] and taking into account that $k=1000$.

As an example of the circuit behavior, a Poincaré section and the trend of the state variable $x(\tau)$, obtained experimentally from our circuit, are shown in Fig. 6. The parameters of the model have been chosen so that a SNA appears. In particular, they have been chosen according to Ref. 9 as follows: $\varepsilon_1=0.08$, $\varepsilon_2=1$, $\omega=(\sqrt{5}+1)/2$, $\varepsilon=5.075$.

IV. ANALYSIS OF THE EXPERIMENTAL DATA

Both implemented circuits show a transition from quasiperiodic motion to SNAs when the amplitude of the two waveform generators used to build the signal $F(\tau)$ is varied, i.e., when the parameter ε is changed. To characterize this transition, we recorded the trends of the state variables of the two circuits for different values of the parameter ε and applied the method described in Sec. II. All the data have been acquired by using a data acquisition board (National Instruments AT-MIO 1620E) with a sampling frequency $f_s=200$ kHz for $T=2s$ (i.e., 400 000 samples for each time series). In all the acquisitions, we set $f_1=\Omega_1/2\pi=159.00$ Hz and $f_2=\Omega_2/2\pi=98.36$ Hz. The other parameters have been chosen as discussed in Sec. III. In particular, for circuit 1 we vary ε from $\varepsilon=0.01$ to $\varepsilon=0.1$ at steps of 0.001. This corresponds to varying the peak-to-peak amplitude of the two waveform generators from 20 to 200 mV at

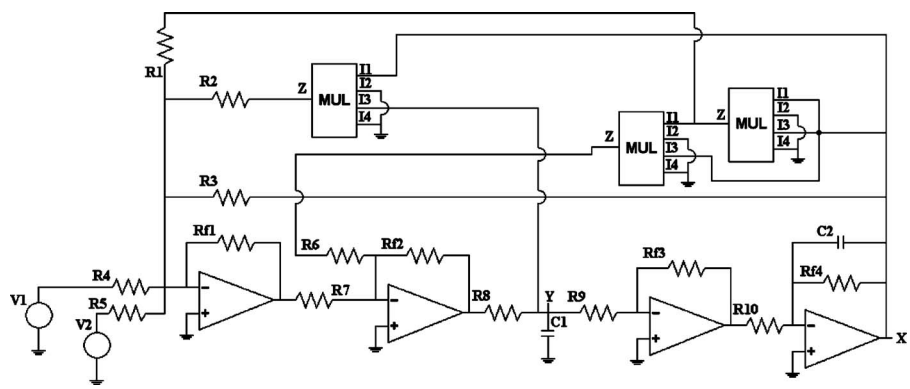

FIG. 5. Circuit 2: SNA circuit implementing Eq. (11) with $R_1=1$ kΩ, $R_2=1$ kΩ, $R_3=10$ kΩ, $R_4=10$ kΩ, $R_5=10$ kΩ, $R_6=1$ kΩ, $R_7=100$ kΩ, $R_8=1$ kΩ, $R_9=100$ kΩ, $R_{10}=22$ kΩ, $R_{f1}=10$ kΩ, $R_{f2}=100$ kΩ, $R_{f3}=100$ kΩ, $R_{f4}=100$ kΩ, $C_1=210$ nF, and $C_2=13$ nF.

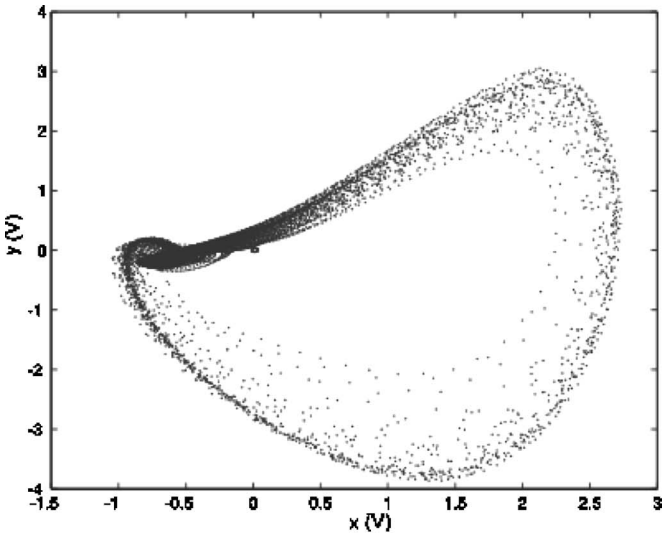

(a)

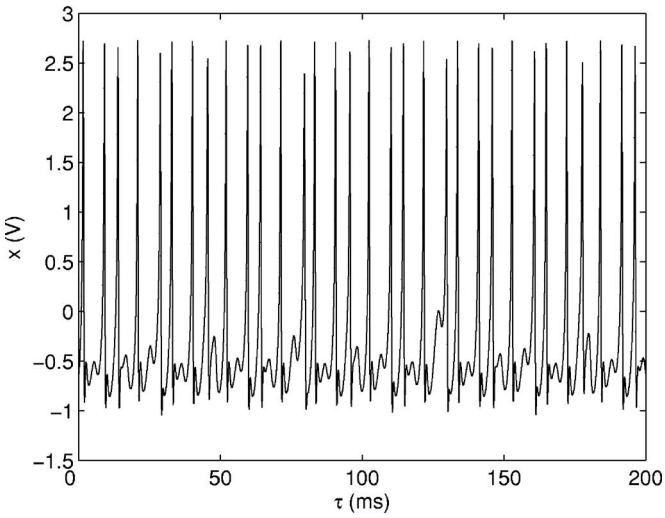

(b)

FIG. 6. Experimental results for Circuit 2 with $\varepsilon=5.075$. (a) Poincaré section of the strange nonchaotic attractor in the phase plane $x-y$; (b) trend of the state variable $x(\tau)$.

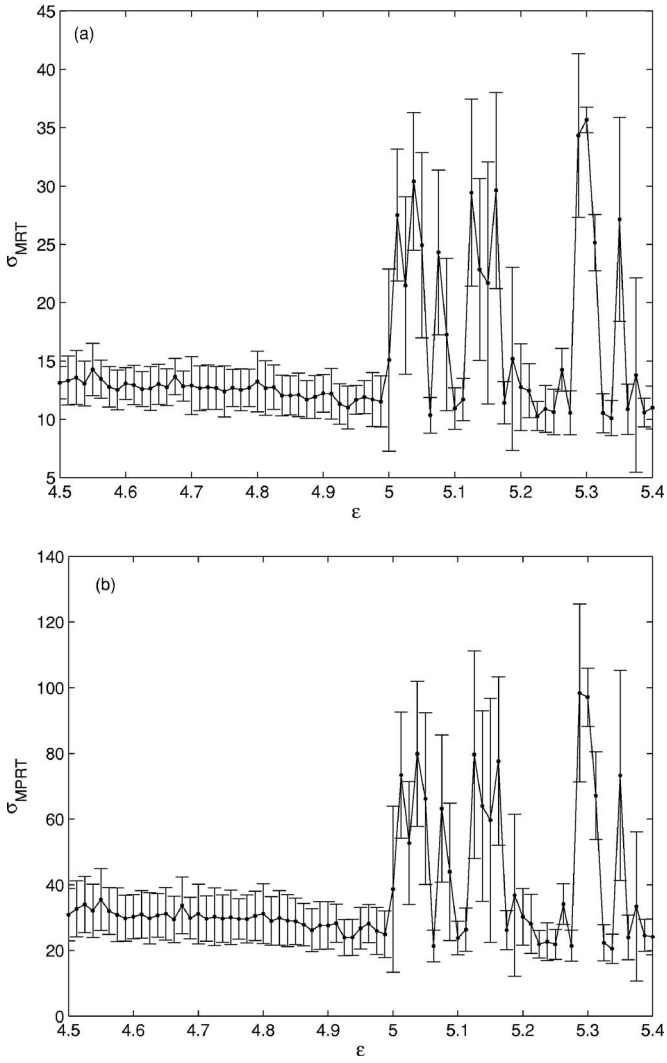

FIG. 7. Variances of the recurrence measures computed on experimental data of the semiconductor laser system with the threshold $\delta=0.04\sigma$, where σ is the standard deviation of the data. (a) Variance of T_{MRT}; (b) variance of N_{MPRT}. In fact, the mean values of σ_{MRT} and σ_{MPRT} are plotted and the corresponding standard deviation over different trajectories of 50 000 data points and 500 as the length of each segment are plotted.

steps of 2 mV and allows us to have a large enough number of data points to perform the analysis described in Sec. II.

As concerns circuit 2, we vary the parameter ε from $\varepsilon=4.5$ to $\varepsilon=5.5$. Consequently, the peak-to-peak amplitude of the waveform generators (which is equal to $V_{pp}=2\varepsilon_1\varepsilon$) varies from 720 to 880 mV at steps of 2 mV.

The measures of complexity defined in Sec. II have then been applied to analyze these experimental data. Because the variances of T_{MRT} and N_{MPRT} detect the transitions better than T_{MRT} and N_{MPRT}, we present, respectively, their behavior in Figs. 7 and 8 for the semiconductor laser system and the VdP–FHN model. From these figures, one can see that the experimental results (Fig. 7) match closely with the numerical ones in the semiconductor laser system (Fig. 1). The transition to SNAs is clearly observed in the variances which increase abruptly at the critical value $\epsilon\sim 5$. In the VdP–FHN model, one encounters some changes before the main transition which takes place at $\epsilon\sim 0.034$ (Fig. 8). These changes could be related to the fact that we are dealing with real components and the changes show that the circuit behaves in a slight different manner. When dealing with experiments, noise could also lead to parameter mismatches. However, the main transition to SNAs takes place at $\epsilon\sim 0.034$ and is close to the one of the numerical case at $\epsilon\sim 0.039$ (Fig. 2). The relative error (about 13%) of the result from the experiments is in the order of magnitude of the electronic parameter tolerance (about 10%). In order to plot Figs. 7 and 8, we have done experimentally eight realizations of time series for each value of the bifurcation parameter ϵ and computed σ_{MRT} and σ_{MPRT} for each realization. We then computed, respectively, the mean value and the standard deviation of σ_{MRT} and σ_{MPRT} of the eight realizations for each value of ϵ. Finally, we plotted the mean value versus ϵ. Above and below the mean value, the corresponding standard deviation is plotted. We see clearly that the changes of the measures of complexity are well above the error bars. The number of realizations is not large. However, when dealing with experiments, one

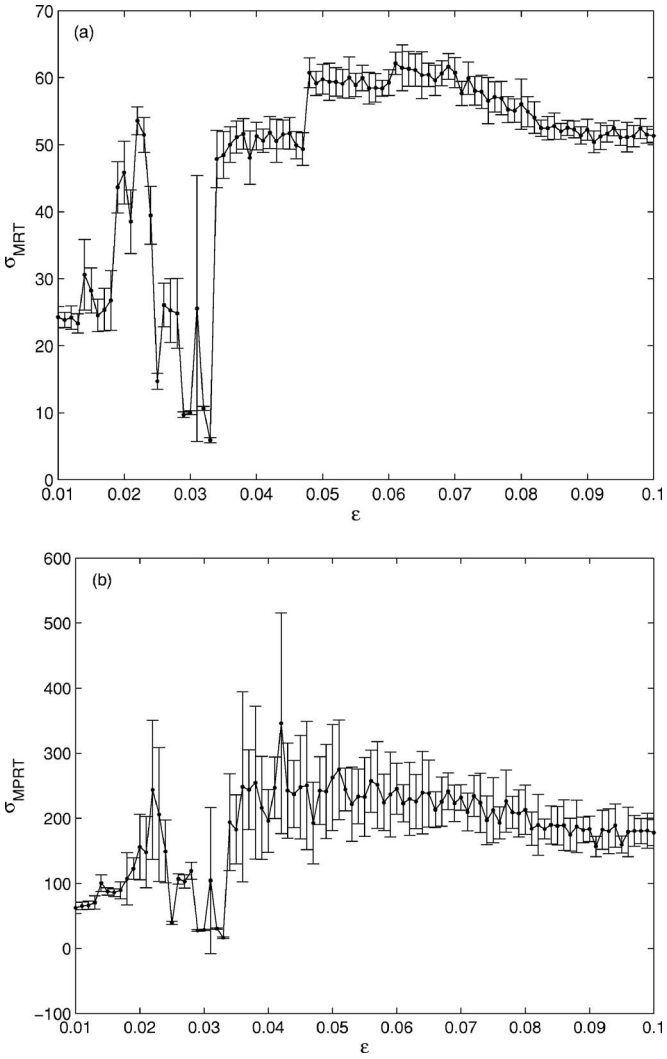

FIG. 8. Variances of the recurrence measures computed on experimental data of the VdP-FHN system with the threshold $\delta=0.04\sigma$, where σ is the standard deviation of the data. (a) Variance of T_{MRT}; (b) variance of N_{MPRT}. In fact, the mean values of σ_{MRT} and σ_{MPRT} are plotted and the corresponding standard deviation over different trajectories of 50 000 data points and 500 as the length of each segment are plotted.

encounters some difficulties and it is not always easy to generate as many realizations as one would wish in order to make an even more precise computation.

Note that, in all the computations, the real coordinates have been used. This does not mean that, if only one observable of the system is available, as it usually is in nature, the recurrence analysis could not be done. In that case, one could use the delay embedding technique[28] and then perform the analysis. However, the embedding parameters should be chosen carefully and appropriately to the system under study to avoid spurious structures in the RP that could influence the analysis. We wish also to mention that, in this study we know *a priori* where the transitions to SNAs take place and the recurrence measures indicate these transitions rather well. If it happens that one has only observations at a fixed value of the bifurcation parameter and wishes to infer in which state the system is, this is still possible using recurrence techniques. The work done in Refs. 16 and 17 gives reliable criteria to recognize quasiperiodic dynamics. The computation of the recurrence measure called Determinism (*DET*) on the main diagonal line of the cross-recurrence plot could show whether the system is in the strange nonchaotic regime.[13,18]

V. SUMMARY

We have applied some recently introduced measures of complexity that are based on the white vertical structures in recurrence plots to detect the transition from quasiperiodic motion to SNAs in continuous systems and experimental data. More precisely, we have studied the transition to SNAs through the intermittency route in two excitable systems, namely a semiconductor laser model with optical feedback and the van der Pol–Fitz Hugh–Nagumo model. The measures of complexity based on the time needed by the system to recur to a neighborhood of a previous point of the trajectory are able to detect the onset of the strange nonchaotic dynamics in the numerically obtained data. The measures fluctuate slightly in the quasiperiodic regime and strongly in the strange nonchaotic one, but at the critical value of the bifurcation parameter there is a drastic jump that makes it easy to identify this bifurcation.

The experimental circuits, based on operational amplifiers, implementing the equations governing the two systems, have been realized and experimental data showing transitions to SNAs have been generated. We have observed a good matching in the behavior of the recurrence measures computed from the numerical and experimental data for the semiconductor laser system. In the van der Pol–Fitz Hugh–Nagumo model, some changes in the variation of the variances of the recurrence measures have been observed before the main transition to SNAs. These changes could be explained by some parameter mismatches introduced by the electronic implementation.

We hope that this work will add a contribution to all the works done up to now in order to observe SNAs in experiments. We also expect that the potentials of RPs for applications will be increased and that the recurrence quantification based on white vertical lines in RPs will find applications in other fields of life science.

ACKNOWLEDGMENTS

The authors would like to acknowledge the support of EU under the COST Action B27 ENOC and SFB 555 (DFG). We thank Dr. M. C. Romano and Dr. M. Thiel for very useful suggestions and a careful reading the manuscript. A.P. thanks DST, Government of India for support.

[1] M. C. Cross and P. C. Hohenberg, "Pattern formation outside of equilibrium," Rev. Mod. Phys. **65**, 851 (1993).
[2] S. C. Müller, P. C. Coullet, and D. Walgraef, "From oscillations to excitability: A case study in spatially extended systems," Chaos **4**, 439 (1994).
[3] F. T. Arecchi, L. Fortuna, M. Frasca, R. Meucci, and G. Sciuto, "A programmable electronic circuit for modelling CO_2 laser dynamics," Chaos **15**, 043104 (2005).
[4] M. C. Eguia, G. B. Mindlin, and M. Giudici, "Low-frequency fluctuations in semiconductor lasers with optical feedback are induced with noise," Phys. Rev. E **58**, 2636 (1998).
[5] B. Lindner, J. Garcia–Ojalvo, A. Neiman, and L. Schimansky-Geier, "Effects of noise in excitable systems," Phys. Rep. **392**, 321 (2004), and references therein.

[6]A. S. Pikovsky, and J. Kurths, "Coherence resonance in a noise-driven excitable system," Phys. Rev. Lett. **78**, 775 (1997).
[7]C. Grebogi, E. Ott, S. Pelikan, and J. A. Yorke, "Strange attractors that are not chaotic," Physica D **13**, 261 (1984).
[8]A. J. Mandell and A. Selz, "Brain stern neuronal noise and neocortical resonance," J. Stat. Phys. **70**, 355 (1993).
[9]A. Prasad, B. Biswal, and R. Ramaswamy, "Strange nonchaotic attractors in driven excitable systems," Phys. Rev. E **68**, 037201 (2003).
[10]G. Ruiz and P. Parmananda, "Experimental observation of strange nonchaotic attractors in a driven excitable system," Phys. Lett. A **367**, 478 (2007).
[11]U. Feudel, J. Kurths, and A. Pikovsky, "Strange nonchaotic attractor in a quasiperiodically forced circle map," Physica D **88**, 176 (1995).
[12]U. Feudel, S. Kuznetsov, and A. Pikovsky, *Strange Nonchaotic Attractors: Dynamics between Order and Chaos in Quasiperiodically Forced Systems*, World Scientific Series on Nonlinear Science, Series A (World Scientific, Singapore, 2006), Vol. 56.
[13]N. Marwan, M. C. Romano, M. Thiel, and J. Kurths, "Recurrence plots for the analysis of complex systems," Phys. Rep. **438**, 237 (2007).
[14]M. Thiel, M. C. Romano, and J. Kurths, "Analytical description of recurrence plots of white noise and chaotic processes," Appl. Nonlin. Dyn. **11**, 2030 (2003).
[15]J. B. Gao, "Recurrence time statistics for chaotic systems and their applications," Phys. Rev. Lett. **83**, 3178 (1999).
[16]Y. Zou, D. Pazo, M. C. Romano, M. Thiel, and J. Kurths, "Distinguishing quasiperiodic dynamics from chaos in short time series," Phys. Rev. E **76**, 016210 (2007).
[17]Y. Zou, M. Thiel, M. C. Romano, and J. Kurths, "Analytical description of recurrence plots of dynamical systems with non-trivial recurrences," Int. J. Bifurcation Chaos Appl. Sci. Eng. **17**, 4273 (2007).
[18]E. J. Ngamga, A. Nandi, R. Ramaswamy, M. C. Romano, M. Thiel, and J. Kurths, "Recurrence analysis of strange nonchaotic dynamics," Phys. Rev. E **75**, 036222 (2007).
[19]J. P. Eckmann, S. O. Kamphorst, and D. Ruelle, "Recurrence plots of dynamical systems," Europhys. Lett. **4**, 973 (1987).
[20]M. Thiel, M. C. Romano, J. Kurths, R. Meucci, E. Allaria, and F. T. Arecchi, "Influence of observational noise on the recurrence quantification analysis," Physica D **171**, 138 (2002).
[21]A. M. Yacomotti, M. C. Eguia, J. Aliaga, O. E. Martinez, and G. B. Mindlin, "Interspike time distribution in noise driven excitable systems," Phys. Rev. Lett. **83**, 292 (1999).
[22]M. Guidici, C. Green, G. Giacomelli, U. Nespolo, and J. Tredicce, "Andronov bifurcation and excitability in semiconductor lasers with optical feedback," Phys. Rev. E **55**, 6414 (1997).
[23]A. C. Scott, "The electrophysics of a nerve fiber," Rev. Mod. Phys. **47**, 487 (1975).
[24]T. Yang and K. Bilimgut, "Experimental results of strange nonchaotic phenomenon in a second-order quasi-periodically forced electronic circuit," Phys. Lett. A **236**, 494 (1997).
[25]A. Venkatesan, K. Murali, and M. Lakshmanan, "Birth of strange nonchaotic attractors through type III intermittency," Phys. Lett. A **259**, 246 (1999).
[26]K. Thamilmaran, D. V. Senthilkumar, A. Venkatesan, and M. Laksmanan, "Experimental realization of strange nonchaotic attractors in a quasiperiodically forced electronic circuit," Phys. Rev. E **74**, 036205 (2006).
[27]A. S. Sedra and K. C. Smith, *Microelectronic Circuits* (Oxford University Press, New York, 2003).
[28]F. Takens, *Dynamical Systems and Turbulence*, Lecture Notes in Mathematics Vol. 898 (Springer, Berlin, 1981), p. 366.